

# Radiation Absorbed Dose Estimates for Indium-111-Labeled B72.3, an IgG Antibody to Ovarian and Colorectal Cancer: MIRDO Dose Estimate Report No. 18

George Mardirossian, A. Bertrand Brill, Steven J. Harwood, John Olsen, Karen A. Dwyer and Jeffry A. Siegel  
*Department of Nuclear Medicine, University of Massachusetts Medical Center, Worcester, Massachusetts; Bay Pines Veterans Administration Hospital, Tampa, Florida; Ohio State University, Columbus, Ohio; Cytogen, Inc., Princeton, New Jersey; and Department of Radiation Oncology, Cooper Hospital/University Medical Center, Camden, New Jersey*

**Key Words:** indium-111-labeled B72.3; colorectal cancer; ovarian cancer; MIRDO dose estimate report

**J Nucl Med 1998; 39:671-676**

The estimated absorbed doses from  $^{111}\text{In}$ -labeled B72.3 (OncoScint; Cytogen, Inc., Princeton, NJ) administered by intravenous administration are given in Table 1. The data and assumptions used for the calculations follow.

Received Jan. 27, 1997; revision accepted Jun. 12, 1997.

For correspondence or reprints contact: George Mardirossian, PhD, University of Massachusetts Medical Center, Department of Nuclear Medicine, 55 Lake Avenue North, Worcester, MA 01655.

## Radiopharmaceutical

OncoScint CR/OV, a radioimmunodiagnostic agent developed by Cytogen, Inc., is an IgG antibody that targets the TAG-72 antigen. The antibody B72.3 was labeled with  $^{111}\text{In}$  through a linker GYK-DTPA (1) and the conjugate B72.3-GYK-DTPA is designated as CYT 103. The labeled antibody binds to a carbohydrate epitope on the TAG-72 antigen (2). Immunohistological results demonstrate that B72.3 reacts with the majority of ovarian and colon adenocarcinomas, but does not react substantially with a wide spectrum of normal human tissues (3-6). In 1993, the agent was approved by the Food and Drug Administration for use in the diagnosis of colorectal cancer. This is what provided the rationale for a MIRDO dose

**TABLE 1**  
 Estimated Absorbed Dose from Intravenous Administration of Indium-111 OncoScint\*

Organ	Men (n = 6)			Women (n = 7)		
	$^{111}\text{In}$	$^{114\text{m}}\text{In}^\dagger$	Total	$^{111}\text{In}$	$^{114\text{m}}\text{In}^\dagger$	Total
Adrenals	0.25	0.002	0.25	0.29	0.002	0.30
Brain	0.07	0.002	0.07	0.08	0.002	0.08
Breasts				0.10	0.002	0.10
Gallbladder wall	0.30	0.002	0.30	0.36	0.002	0.36
Lower large intestine wall	0.31	0.006	0.31	0.37	0.007	0.38
Small intestine	0.17	0.001	0.18	0.20	0.002	0.20
Stomach	0.15	0.002	0.15	0.18	0.002	0.19
Upper large intestine wall	0.23	0.003	0.24	0.28	0.003	0.29
Heart wall	0.36	0.005	0.36	0.43	0.010	0.44
Kidneys	0.42	0.019	0.44	0.50	0.014	0.52
Liver	0.63	0.034	0.67	0.94	0.059	1.00
Lungs	0.27	0.004	0.27	0.35	0.010	0.36
Muscle	0.11	0.002	0.11	0.12	0.002	0.12
Ovaries				0.19	0.002	0.20
Pancreas	0.23	0.002	0.23	0.29	0.002	0.29
Red marrow	0.59	0.043	0.63	0.54	0.037	0.57
Bone surfaces	0.29	0.009	0.30	0.31	0.010	0.32
Skin	0.06	0.002	0.06	0.07	0.002	0.07
Spleen	0.55	0.027	0.58	1.01	0.066	1.08
Testes	0.14	0.014	0.15			
Thymus	0.14	0.002	0.14	0.15	0.002	0.15
Thyroid	0.09	0.002	0.09	0.09	0.002	0.10
Urinary bladder wall	0.14	0.002	0.14	0.16	0.003	0.16
Uterus				0.15	0.002	0.16
Total body	0.14	0.004	0.14	0.16	0.004	0.17

\*Absorbed dose per unit administered activity of  $^{111}\text{In}$  (mGy/MBq).

$^\dagger$ 0.0006 MBq of  $^{114\text{m}}\text{In}$  and  $^{114}\text{In}$ /MBq of  $^{111}\text{In}$ .

1 mGy/MBq = 3.7 rad/mCi.

**TABLE 2**  
Nuclear Data of Indium Radioisotopes Used in This Work

Radionuclides Physical half-life Decay mode	<sup>111</sup> In 2.83 days EC				<sup>114</sup> In 71.9 sec β <sup>-</sup> (99.5%) IT (95.7%)				<sup>114m</sup> In 49.51 days EC (4.3%)			
	E <sub>i</sub>	n <sub>i</sub>	Δ <sub>i</sub>		E <sub>i</sub>	n <sub>i</sub>	Δ <sub>i</sub>		E <sub>i</sub>	n <sub>i</sub>	Δ <sub>i</sub>	
Principal radiation	keV	rad g/(μCi hr)	Gy kg/(Bq sec)	keV	rad g/(μCi hr)	Gy kg/(Bq sec)	keV	rad g/(μCi hr)	Gy kg/(Bq sec)	keV	rad g/(μCi hr)	Gy kg/(Bq sec)
γ	171.3	0.902	0.329	2.48E-14	1300	0.0014	0.00388	2.92E-16	190.3	0.154	0.0625	4.69E-15
γ	245.3	0.94	0.491	3.70E-14	558	0.00067	0.0008	6.01E-17	558.4	0.044	0.0522	3.92E-15
γ					576	0.00004	0.000048	3.62E-18	725.2	0.043	0.0669	5.03E-15
x-ray	23-27	0.826	0.042	3.13E-15	23-27	0.00361	0.00018	1.37E-17	24-28	0.363	0.019	1.43E-15
Nonpenetrating			0.074	5.56E-15			1.65	1.24E-13			0.303	2.27E-14

E<sub>i</sub> = the mean energy per particle or photon; n<sub>i</sub> = the number of particles or photons per nuclear transition; Δ<sub>i</sub> = the mean energy emitted per nuclear transition. Nonpenetrating radiation includes conversion and Auger electrons.

estimate report. The committee plans to release reports on other approved labeled antibody products as data are made available.

Indium-111-Cl<sub>3</sub> was buffered with 0.5 M sodium acetate (pH = 6.0) before mixing in a shielded vial with the antibody. The preparation was allowed to stand for 30 min at room temperature and filtered with a 0.22 μm Millex GV filter before administration. Labeling efficiency was typically over 95% as determined by instant thin-layer chromatography. The maximum amount of <sup>114m</sup>In at the expiration date was 0.16%, and typically was < 0.06% at the time of injection. This value was used in the dose calculations. Each of the 13 colorectal carcinoma patients discussed in this article (7 women, average weight 75 kg, range 45-150 kg; 6 men, average weight 79 kg,

range 64-96 kg) received approximately 185 MBq (5 mCi) <sup>111</sup>In with 1 mg of antibody intravenously.

### Nuclear Data

The nuclear data for <sup>111</sup>In, <sup>114</sup>In and <sup>114m</sup>In are given in Table 2. These are based on the MIRDO Radionuclide Data and Decay Schemes (7). Nonpenetrating dose contributions come from long-lived <sup>114m</sup>In, which is a contaminant in commercial <sup>111</sup>In products.

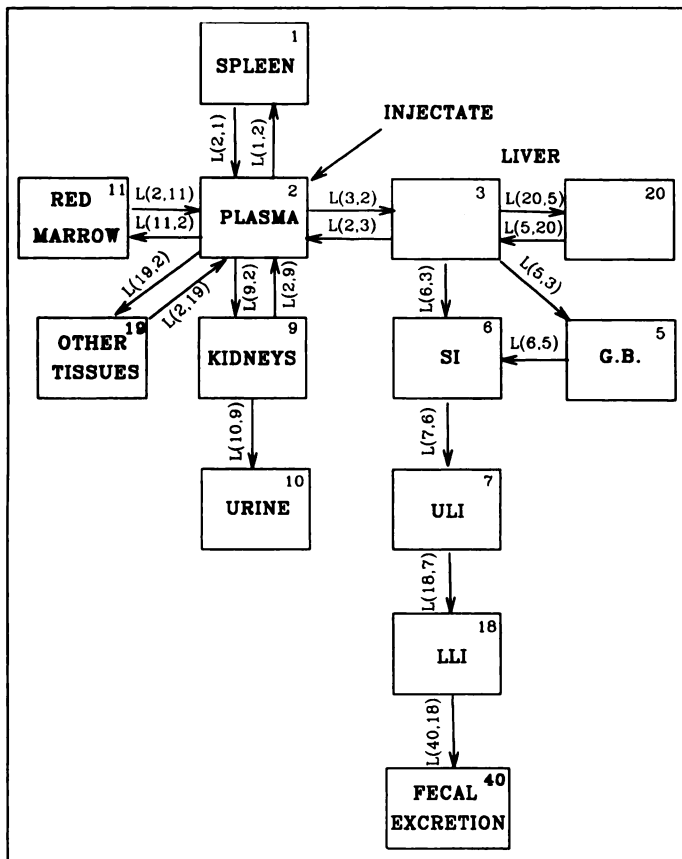


**FIGURE 1.** Compartmental model of system used for estimating the time-activity curve distribution of the gastrointestinal tract organs. SI = small intestine; G.B. = gallbladder; ULI = upper large intestine; LLI = lower large intestine.

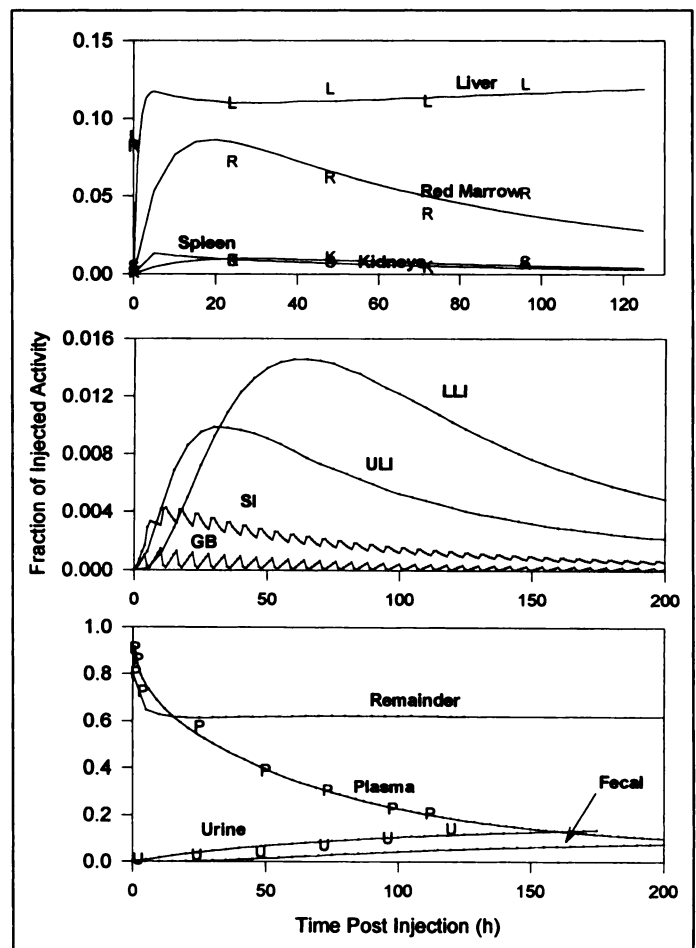


**FIGURE 2.** Time-activity curves of a typical patient (Patient 1) as obtained from the compartmental analysis of Figure 1. Data points are indicated by letters: L = liver; R = red marrow; S = spleen; K = kidneys; P = plasma; U = urine; GB = gallbladder; ULI = upper large intestine; LLI = lower large intestine; SI = small intestine.

## Biologic Data

Biodistribution data were obtained from colorectal cancer patients after the administration of diagnostic amounts of activity of  $^{111}\text{In}$ -CYT-103 (OncoScint CR/OV). The data were obtained from external imaging studies conducted at three medical institutions: the University of Massachusetts Medical Center (UMMC) (4 patients); Bay Pines Veterans Administration Hospital (BPVA) (6 patients); and Ohio State University Hospital (OSU) (3 patients), for a total of 13 patients.

Sequential biodistribution studies (up to 7–10 days postinjection) were performed, including blood (serum) clearance, whole-body retention and organ activity contents (serum, liver, lung, spleen, kidneys, testes and red marrow). Measurements were made using a quantitative conjugate emission imaging protocol along with transmission imaging and a thickness-dependent camera with sensitive calibration (8). The amount of  $^{111}\text{In}$  excreted in the urine was measured but stool collections were not obtained. All data analysis was done at the UMMC using calibration factors specific for each of the patient study cameras determined through a common protocol followed at each of the centers.

The fraction of the injected dose in source organs was determined from data received from each site by drawing regions of interest (ROIs) about the specified source organs. ROIs identified at early imaging sessions were linked to each other and moved as a group so that interorgan spatial relations were maintained; interorgan spatial relations were then used at later times when not all organs were clearly visualized. The activity in each source organ ROI was calculated after background subtraction at each measurement time. Counts per pixel in a background ROI, selected in the lower abdomen, were subtracted from each pixel in the source organ ROI. Serum clearance and urine excretion data were established by serum, urine and standards counted at the end of the sample collection period. Organ data were quantitated after correction for physical decay.

To evaluate the contribution of gastrointestinal (GI) excretion to absorbed dose estimates, calculations were made using the model proposed by Stabin (9). Since stool losses were not measured, fecal excretion was estimated by compartmental analyses for four patients (two men and two women). In this model, the blood compartment communicates bidirectionally with the liver, which connects unidirectionally to the GI tract. Passage through the GI tract was estimated using the International Commission on Radiation Protection transit time model (10), which assigns typical values for transit rates to the small intestine (SI), upper large intestine (ULI) and lower large intestine (LLI) as 0.25, 0.075 and 0.0417  $\text{hr}^{-1}$ , respectively (11). The general model (Fig. 1) describes the liver as two compartments that distribute 70% and 30% of its activity to the SI and gallbladder, respectively. The gallbladder empties its contents over a 2-hr period (contraction) to the SI at 6-hr intervals (12). The residence times in the various segments of the GI tract were entered into the MIRDOSE2 computer software program and treated as source organs (13).

The testicular region was included in the field of view in planar views of the pelvis for four of the six male patients. In the absence of adequate transmission data, testicular content was calculated from the geometric mean of the imaged uptake, and a 3-in. organ thickness was assumed for attenuation correction (mean of two measurements at 2 in. and 4 in.).

The source organs included in the study were the liver, spleen, kidneys, testes, bone marrow, heart chamber, lungs, urinary bladder contents and the remainder of the body along with gallbladder contents (LLI, SI and ULI). The total content

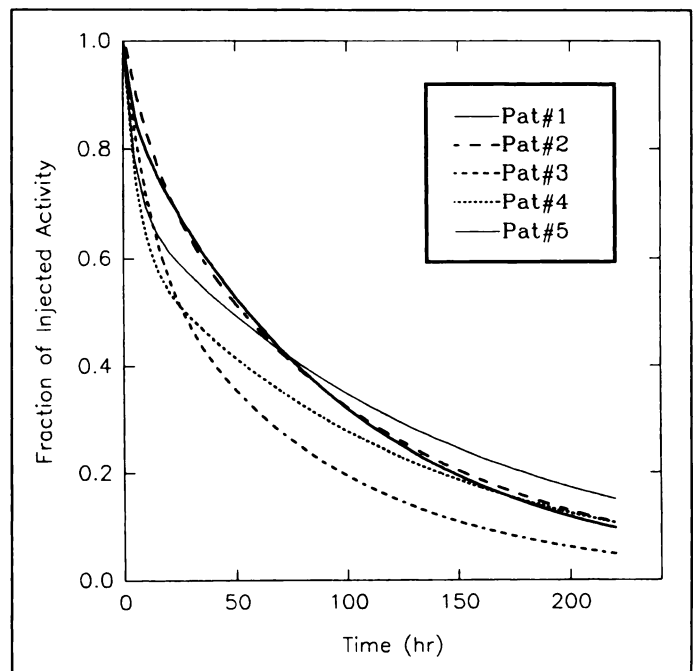


FIGURE 3. Plasma clearance curves (UMMC patients).

of radioactivity in the bone marrow was estimated from measurements over two lumbar vertebrae (region L2–L4) multiplied by a factor (22.5) (14). This factor scales the sampled activity to total marrow content. The remainder of the body activity at each sampling period was considered to be 100% of the injected activity minus the sum of all activities otherwise accounted for in the measured source organs (including fecal activity) and activity lost in urine. The partition of plasma activity included an assignment of 10% of the plasma pool to the heart and lungs, respectively (15).

The fraction of injected activity in each source organ was calculated for each measurement site and time for each of the patients. Best-fit parameters for a three-component exponential function were obtained for each patient using the CONSAM program (16) (Model Type 2). In this model, the values of the exponentials for the different measurements for each individual patient were the same for all organs (GI tract not included). Only the coefficients of the three terms varied within a given patient (17). The strongest determinants of the exponentials values were the blood and whole-body activity measurements. Blood contents of the different organs were based on standard male-to-female blood volume as indicated in Poston et al. (15). CONSAM was also used to solve the compartmental model presented in Figure 1 to estimate GI tract organ contents. Urinary excretion and bladder residence times were modeled assuming five voids per day, with 4.8 hr voiding intervals. Figure 2 presents time-activity curves for a typical patient (Patient 1) for measured source organs and the GI tract along with computer best-fit values.

## Radiation Absorbed Dose

The area under the respective time-activity curves and residence times were calculated for each organ. Values for each patient were entered separately into the MIRDOSE2 program (using the MIRD formalism) (13,18) using reference male/female phantoms (19,20). Plasma clearance data are plotted in Figure 3. Table 3 lists the best-fitting model parameters for each of the body regions measured for each of the 13 patients studied. The derived parameters from the computer fit data for plasma and the different source organs in Table 3 reveal a wide

**TABLE 3**  
Best-Fit Model Parameters for Individual Patients by Source Organs

Organ	Parameter ( $\theta$ )	Bay Pines Veterans Administration Hospital					University of Massachusetts Medical Center					Ohio State University				
		M (90 kg) Patient 1	M (75 kg) Patient 2	M (96 kg) Patient 3	F (83 kg) Patient 4	M (73 kg) Patient 5	F (69 kg) Patient 5B	F (56 kg) Patient 2	M (64 kg) Patient 3	F (45 kg) Patient 5	F (67 kg) Patient 6	M (73 kg) Patient 6	F (150 kg) Patient 8	F (53 kg) Patient 11		
Serum	$\lambda_1$	1.50E+00	5.20E-02	2.38E-02	4.86E-02	7.23E-03	2.18E-01	1.36E-02	2.26E-01	1.87E-02	1.03E-01	2.02E-01	1.03E-01	3.35E-02		
	$\lambda_2$	1.93E-02	4.12E-03	5.00E-02	1.17E-02	9.00E-03	1.23E-02	2.76E-02	6.49E-03	1.00E-04	1.69E-02	1.33E-02	3.28E-02	8.29E-03		
	$\lambda_3$	5.00E-04	1.00E-04	5.89E-04	1.00E-04	1.00E-04	1.63E-03	1.24E-03	6.61E-04	2.42E-03	5.00E-04	4.44E-03	5.91E-03	1.00E-04		
Whole body	$\alpha_1$	1.86E-01	3.83E-01	1.00E-00	1.41E-01	-4.49E-02	2.28E-01	-3.98E-01	1.35E-01	1.00E-00	7.08E-01	-4.00E-03	-4.00E-03	4.39E-01		
	$\alpha_2$	6.79E-01	1.00E-00	-1.94E-02	7.66E-01	9.03E-01	8.75E-01	1.00E+00	1.00E+00	6.31E-01	1.77E-01	5.47E-01	5.47E-01	5.40E-01		
	$\alpha_3$	1.37E-01	-3.86E-01	2.17E-03	7.95E-02	1.16E-01	-7.09E-02	3.83E-01	-1.63E-01	-6.48E-01	-1.34E-02	4.43E-01	4.43E-01	2.45E-02		
Liver	$\alpha_1$	-1.04E-02	5.41E-02	3.61E-02	-2.55E-02	3.87E-01	9.24E-02	-3.93E-02	8.07E-02	-2.76E-02	5.78E-02	-1.16E-01	1.00E+00	-7.33E-02		
	$\alpha_2$	2.35E-01	3.00E-01	-3.62E-02	1.29E-01	-1.15E-01	-3.18E-02	4.69E-02	-8.07E-02	2.12E-02	1.81E-01	1.00E+01	-1.00E+00	1.91E-01		
	$\alpha_3$	7.75E-01	6.54E-01	1.00E-00	8.98E-01	7.32E-01	9.74E-01	1.00E+00	1.00E+00	1.00E+00	7.79E-01	1.00E-01	1.00E+00	8.81E-01		
Spleen	$\alpha_1$	-1.47E-02	-4.44E-02	-5.73E-01	-9.04E-02	8.93E-01	-6.26E-02	-1.66E-01	-7.71E-03	-6.72E-03	-1.55E-01	5.85E-02	1.55E-01	-8.67E-02		
	$\alpha_2$	2.53E-02	-6.90E-02	3.59E-01	-1.26E-01	-9.45E-01	-1.30E-02	6.72E-02	-1.62E-01	4.26E-01	-8.32E-03	-4.35E-01	-5.33E-01	7.74E-02		
	$\alpha_3$	1.28E-01	2.11E-01	3.71E-01	1.72E-01	1.52E-01	1.81E-01	2.30E-01	2.51E-01	-3.18E-01	2.88E-01	5.44E-01	4.43E-01	3.36E-01		
Kidney	$\alpha_1$	-4.40E-03	4.13E-03	1.37E-02	-6.77E-03	1.35E-01	-1.80E-02	6.04E-03	-1.48E-02	-5.42E-03	-1.77E-02	4.03E-02	7.28E-02	-6.57E-02		
	$\alpha_2$	1.43E-03	-7.37E-03	-1.47E-02	-6.36E-03	-1.19E-01	1.80E-02	-7.55E-03	2.60E-02	6.37E-02	2.16E-02	-1.17E-03	-1.37E-01	1.51E-01		
	$\alpha_3$	7.97E-03	2.08E-02	1.79E-02	2.64E-02	1.41E-02	5.08E-03	2.06E-02	-4.28E-03	-5.08E-02	6.57E-03	1.19E-01	8.78E-02	1.05E-02		
Red marrow	$\alpha_1$	-1.05E-02	-1.00E-02	3.47E-02	-1.38E-02	1.44E-01	-2.94E-02	4.01E-02	-5.82E-03	-6.64E-02	-1.23E-02	4.55E-03	7.59E-02	-6.73E-03		
	$\alpha_2$	4.37E-03	3.87E-02	-1.87E-02	1.42E-02	-1.12E-01	4.85E-02	-3.73E-02	1.19E-02	-1.31E-01	1.75E-02	-5.81E-02	-1.64E-02	5.44E-02		
	$\alpha_3$	7.12E-03	-6.53E-03	9.06E-03	1.16E-02	-7.24E-03	7.26E-04	1.46E-02	4.90E-02	2.00E-01	6.09E-01	1.04E-01	1.64E-01	1.78E-02		
Testes	$\alpha_1$	-1.00E-02	-2.59E-02	-3.60E-02	-1.75E-01	-6.41E-01	2.67E-02	-1.07E-01	-1.23E-02	1.88E-02	-2.59E-01	2.20E-01	1.74E-01	-2.69E-01		
	$\alpha_2$	5.77E-02	2.59E-01	1.30E-01	1.84E-01	8.62E-01	-1.01E-01	3.69E-02	-1.05E-01	1.26E-01	2.59E-01	-6.07E-01	-6.04E-01	1.00E+00		
	$\alpha_3$	3.43E-02	1.94E-02	2.25E-01	1.71E-01	1.43E-01	2.79E-01	2.40E-01	-1.05E-01	-1.05E-01	5.62E-02	1.00E+00	4.40E-01	-1.47E-01		
	$\alpha_1$		-1.55E-04	5.20E-03		-5.36E-03		-1.95E-04								
	$\alpha_2$		-9.23E-05	-4.83E-03		4.52E-03		-3.78E-03								
	$\alpha_3$		3.01E-04	1.21E-04		1.06E-03		4.97E-03								

$\lambda_i$  = exponential coefficients ( $hr^{-1}$ ).  
 $\alpha_i$  = fraction of injected activity parameters.

**TABLE 4**  
Best-Fit Gastrointestinal Tract Parameters

Parameter	Rate Coefficient (hr <sup>-1</sup> )			
	Male Patient 3	Male Patient 1	Female Patient 6	Female Patient 5B
L(2, 3)	0.463	0.763	0.100	0.537
L(3, 2)	0.058	0.114	0.150	0.137
L(20, 3)	0.014	0.013	0.014	0.014
L(3, 20)	0.000	0.000	0.000	0.000
L(6, 3)	0.006	0.007	0.007	0.018
L(6, 5)*	1.800	1.800	1.800	1.800
L(7, 6)*	0.250	0.250	0.250	0.250
L(18, 7)*	0.077	0.077	0.077	0.077
L(40, 18)*	0.042	0.042	0.042	0.042
L(9, 2)	0.240	0.020	0.006	0.042
L(2, 9)	10.000	1.000	0.000	0.603
L(10, 9)	0.140	0.140	0.050	0.028
L(2, 1)	0.089	0.064	0.010	0.228
L(1, 2)	0.003	0.001	0.002	0.009
L(11, 2)	0.011	0.017	0.050	0.196
L(2, 11)	0.020	0.118	0.030	0.450
L(19, 2)	0.000	0.011	0.030	0.007
L(2, 19)	0.002	0.002	0.002	0.000

\*Fixed parameters.

$$L(5, 3) = 0.4286 \times L(6, 3).$$

Compartments are designated as follows: 1 spleen, 2 plasma, 3 and 20 liver, 5 gallbladder, 6 small intestine, 7 upper large intestine, 9 kidneys, 10 urine, 11 red marrow, 18 lower large intestine, 19 other tissues and 40 fecal.

L(n, p) is the rate at which tracer in compartment n arrives from compartment p.

range of early fast clearance components (50% coefficient of variation) and late slow well-defined clearance parameters (19% coefficient of variation). Table 4 lists the best-fitting GI tract model parameters for four patients (2 men and 2 women) who had complete datasets. The residence times calculated (blood plus organ activity) are given in Table 5 for men and women separately, along with average values. The GI tract residence times used for each patient (men and women) are the mean values of the four patient data (Table 5). By eight days postinfusion, an average of 14.4% of the administered activity (range of 7.1%–25.7%) was estimated for fecal excretion, while

an average of 15% (range 9.0%–27.8%) was excreted in the urine.

Only dose contributions from <sup>111</sup>In and <sup>114m</sup>In were included in this article because the levels of <sup>113m</sup>In and <sup>115m</sup>In were negligible. As a result of its long effective half-life, the <sup>114m</sup>In contaminant contributes approximately 2.5% of the total body dose in both men and women.

The individual organ doses within and between study sites are in reasonable agreement. The greatest variations noted were in the dose to kidneys (range 0.24–1.11 mGy/MBq), red marrow (range 0.24–1.30 mGy/MBq) and spleen (range 0.30–1.01 mGy/MBq). In men, the dose to the testes ranged from 0.08–0.29 mGy/MBq. In many patients the testes were only barely discernible, while in others the activity was clearly visualized.

Dose estimates generated with MIRDOSE2 were found to agree closely with those calculated using S values tabulated in MIRD Pamphlet No. 11. Bone absorbed dose was the only exception; the MIRD Pamphlet No. 11 bone dose was about 50% lower than estimated in MIRDOSE2.

The total body absorbed dose from <sup>111</sup>In-OncoScint was found to be 0.14 mGy/MBq for men and 0.17 mGy/MBq for women. These dose estimates are in accord with the total-body and organ doses listed in the package insert for OncoScint CR/OV (i.e., 0.15 mGy/MBq).

## REFERENCES

- Rodwell JD, Alvarez VL, Lee C, et al. Site-specific covalent modification of monoclonal antibodies. In vivo and in vitro evaluations. *Proc Natl Acad Sci USA* 1986;83:2632–2636.
- Johnson VG, Schlom J, Paterson AJ, Bennett J, Mangani JL, Colcher D. Analysis of a human tumor-associated glycoprotein (TAG-72) identified by monoclonal antibody B72.3. *Cancer Res* 1986;46:3118–3124.
- Cytogen Research Report RR-0468. *Preliminary safety and dose-ranging studies with <sup>111</sup>In CYT-103*. Princeton, NJ: Cytogen Corp.; 1989.
- Cytogen Research Report RR-0510. *Evaluation of pivotal <sup>111</sup>In CYT-103 efficacy data for patients with colorectal carcinoma*. Princeton, NJ: Cytogen Corp.; 1989.
- Jusko WJ. In: Cytogen Research Report RR-0696. *General summary: disposition and pharmacokinetics of intravenously administered antibody conjugate <sup>111</sup>In-CYT-103 in human*. Princeton, NJ: Cytogen Corp.; 1990.
- Waldmann TA, Strober W. Metabolism of immunoglobulins. *Progr Allergy* 1969;13: 1–110.
- Weber DA, Eckerman KF, Dillman LT, Ryman JC. *MIRD radionuclide data and decay schemes*. New York: Society of Nuclear Medicine; 1989.
- Doherty P, Schwinger R, King M, Gionet M. *Distribution and dosimetry of indium-111-labeled F(ab')<sub>2</sub> fragments in humans*. In: Fourth International Radiopharmaceutical Symposium, CONF-851113(DE86010102). Oak Ridge, TN: Oak Ridge Associated Universities; 1985:464–476.

**TABLE 5**  
Average Residence Times t (hr) for Indium-Labeled OncoScint

Organ	<sup>111</sup> In			<sup>114m</sup> In		
	Male n = 6	Female n = 7	Average n = 13	Male n = 6	Female n = 7	Average n = 13
Liver	16.26	19.29	17.89	202.2	256.2	231.2
Spleen	1.91	2.69	2.33	15.6	25.5	20.9
Kidneys	1.95	1.90	1.92	18.0	10.0	14.1
Red marrow	21.68	17.63	19.50	149.3	119.3	133.1
Heart content	3.89	3.55	3.71	10.7	19.3	15.3
Lungs	4.05	3.70	3.86	11.1	20.1	15.9
Urinary bladder content†	0.42	0.40	0.41	1.7	1.6	1.6
Remainder of body	34.81	31.01	32.76	398.7	322.9	357.9
Testes*	0.082–0.113		0.10	1.3–2.2		1.7
Gallbladder	0.10			0.1		
Small intestine	0.37			0.7		
Upper large intestine	1.05			2.4		
Lower large intestine	1.55			4.3		

\*For attenuation thicknesses of 2-in. and 4-in., respectively.

†5 voids/day.

9. Stabin MG. Prediction of radiation dose to the GI tract from analysis of blood and liver time-activity curves. In: Fifth International Radiopharmaceutical Dosimetry Symposium, CONF-910529. Oak Ridge, TN: Oak Ridge Associated Universities; 1992:202-215.
10. International Commission on Radiation Protection Limits for Intake of Radionuclides by Workers. ICRP publication 30. New York: Pergamon Press; 1979:30-34.
11. Eckerman K. Dosimetric methodology of the ICRP. In: Raabe OG, ed. *Internal radiation dosimetry*. Health Physics Society 1994 Summer School. Madison, WI: Medical Physics Publishing; 1994.
12. Mozley PD, Stubbs JB, Kung HF, et al. Biodistribution and dosimetry of iodine-123-IBF: a potential radioligand for imaging the D2 dopamine receptor. *J Nucl Med* 1993;34:1910-1917.
13. Watson E, Stabin MG. Basic alternative software package for internal radiation dose calculations. In: Katheren RL, Higby DP, McKinney MA, eds. *Computer applications in health physics*. Richland, WA: Proceedings of the 17th Midyear Topical Symposium of the Health Physics Society; 1984.
14. Report of the Task Group on Reference Man. ICRP Publication 23. New York: Pergamon Press; 1975.
15. Poston JW, Aissi A, Hui TY, Jimba BM. A preliminary model of the circulating blood for use in radiation dose calculations. In: Fourth International Radiopharmaceutical Dosimetry Symposium, CONF-851113. Oak Ridge, TN: Oak Ridge Associated Universities; 1985:574-586.
16. Berman M, Beltz WF, Greif PC, Chabay R, Boston RC. *CONSAM user's guide*. Bethesda, MD: Laboratory of Mathematical Biology, National Institutes of Health; 1983.
17. Berman M, Schoenfield R. Invariants in experimental data on linear kinetics and the formulation of models. *J Appl Physics* 1956;27:1361-1370.
18. Loevinger R, Budinger TF, Watson EE. *MIRD primer for absorbed dose calculations*. New York: Society of Nuclear Medicine; 1988.
19. Snyder WS, Ford MR, Warner GG. *MIRD Pamphlet No. 5, revised: estimates of specific absorbed fractions for photon sources uniformly distributed in various organs of a heterogeneous phantom*. New York: Society of Nuclear Medicine; 1987.
20. Cristy M, Eckerman KF. *Specific absorbed fractions of energy at various ages from internal photon sources. I. Methods*. ORNL/TM-8381/V1. Oak Ridge, TN: Oak Ridge National Laboratory; 1987.

(continued from page 9A)

**FIRST IMPRESSIONS**  
**An Ectopic Kidney in the Left Axilla**

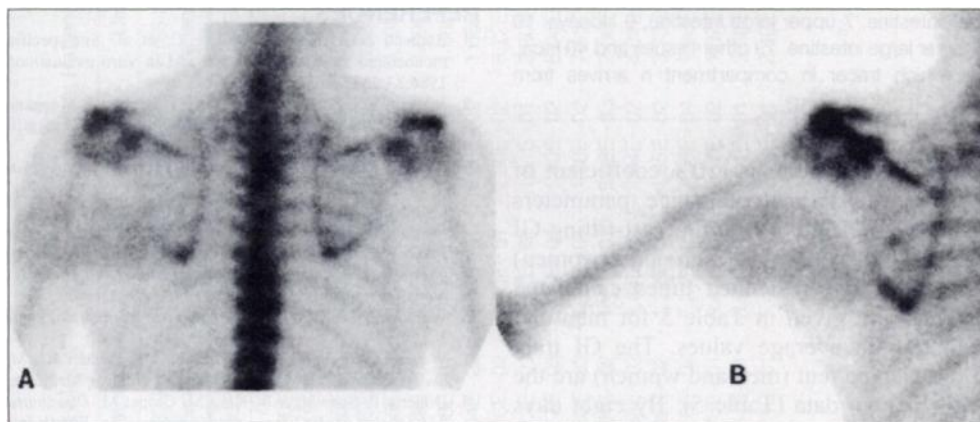


**Figure 1.**

**PURPOSE**

This 50-yr-old man was admitted for slow progression of shortness of breath of 8-mo duration. Chest radiograph showed multiple opacities in the right lung and right-sided pleural effusion. There was a large, hard mass in the left shoulder extending to the axilla. Surgical biopsy revealed a well-differentiated, low-grade fibrosarcoma. Bone scintigraphy imaged a kidney-shaped soft-tissue tumor in the left shoulder region (Fig. 1A, B). No bone involvement was detected.

**TRACER**

Technetium-99m-HDP (800 MBq)

**ROUTE OF ADMINISTRATION**

Intravenous

**TIME AFTER INJECTION**

4 hr

**INSTRUMENTATION**

GE Starcam XRT-4000

**CONTRIBUTORS**

Luban Mrhac, Saad Zakko, Hanan Al-Shamsi and Salha Lootah, Department of Nuclear Medicine, New Dubai Hospital, Dubai, United Arab Emirates